Journal of Molecular Catalysis B: Enzymatic 72 (2011) 282–288

Contents lists available at ScienceDirect

Journal of Molecular Catalysis B: Enzymatic

journal homepage: www.elsevier.com/locate/molcatb

Amperometric xanthine biosensors based on electrodeposition of platinum on polyvinylferrocenium coated Pt electrode

Salih Zeki Baş[a,*], Handan Gülce[b], Salih Yıldız[a]

[a] Department of Chemistry, Selçuk University, Konya 42075, Turkey
[b] Department of Chemical Engineering, Selçuk University, Konya 42075, Turkey

ARTICLE INFO

Article history:
Received 8 April 2011
Received in revised form 24 June 2011
Accepted 24 June 2011
Available online 2 July 2011

Keywords:
Xanthine detection
Xanthine oxidase
Platinum electrodeposition
Amperometric biosensor
Polyvinylferrocenium

ABSTRACT

Novel xanthine biosensors were successfully fabricated by immobilizing xanthine oxidase on polyvinylferrocenium perchlorate matrix ($PVF^+ClO_4^-$) and platinum electrodeposited polyvinylferrocenium perchlorate matrix. $PVF^+ClO_4^-$ film was coated on Pt electrode at +0.7 V vs. Ag/AgCl by electrooxidation of polyvinylferrocene (PVF). Platinum nanoparticles were deposited on $PVF^+ClO_4^-$ electrode by electrochemical deposition in 2.0 mM H_2PtCl_6 solution at −0.2 V. Xanthine oxidase was incorporated into the polymer matrix via ion exchange process by immersing modified Pt electrodes in the enzyme solution. The amperometric responses of the biosensors were measured via monitoring oxidation current of hydrogen peroxide at +0.5 V. Under the optimal conditions, the linear ranges of xanthine detection were determined as 1.73×10^{-3}–1.74 mM for PVF^+XO^- and 0.43×10^{-3}–2.84 mM for PVF^+XO^-/Pt. The detection limits of xanthine were 5.20×10^{-4} mM for PVF^+XO^- and 1.30×10^{-4} mM for PVF^+XO^-/Pt. Moreover, the effects of applied potential, electrodeposition potential, H_2PtCl_6 concentration, amount of electrodeposited Pt nanoparticles, thickness of polymeric film, temperature, immobilization time, xanthine and xanthine oxidase concentrations on the response currents of the biosensors were investigated in detail. The effects of interferents, the operational and storage stabilities of biosensors and the applicabilities to drug samples of the biosensors analysis were also evaluated.

1. Introduction

Xanthine oxidase, controlling a part of purine metabolism and catalyzing the oxidation of hypoxanthine to xanthine and of xanthine to uric acid, plays an important role in human and mammalian life. Xanthine oxidase is a flavoprotein that contains molybdenum, iron and labile sulfur. The enzymatic reaction, occurs between substrate and xanthine oxidase, is based on a mechanism involving nucleophilic attack on substrate by the Mo–OH group at the active site of xanthine oxidase [1]. The levels of xanthine oxidase in clinical disorders related to purine metabolism are symptoms of several diseases such as gout, xanthinuria and hyperuricaemia [2]. In ischemia–reperfusion injury, xanthine oxidase is proposed as a source in the formation of superoxide and hydrogen peroxide in ischemic tissues [3]. For the diagnosis and the treatment of the diseases, the amount of xanthine in the blood and the tissue samples should be easily analyzed. The determination of xanthine is also used in the food industries for the quality control of fish products. Hence, the quantity of xanthine is of clinical and industrial importance [4,5].

In the literature, several analytical methods such as electrophoresis [6,7], HPLC [8,9], amperometric and voltametric methods [10,11] have been reported for quantitative determination of xanthine. In recent years, electrochemical methods have been frequently used for the determination of xanthine and hypoxanthine [4,5,12–14]. Compared with other analytical methods, enzyme-based electrochemical sensors possess simplicity of operation, high sensitivity, and selectivity. In addition to these features, they have advantages such as its ease of use in turbid samples, portability, low cost and fast [4,5]. Generally, the electrochemical detection of xanthine is based on the electrochemical oxidation of the enzymatically generated H_2O_2, or the electrochemical reaction of the introduced redox mediators [11].

Ferrocene derivatives are excellent electron transfer mediators, widely used as mediators to construct mediated amperometric biosensors [15]. Polyvinylferrocenium perchlorate ($PVF^+ClO_4^-$), ferrocene-based redox polymer, is widely used in biosensor applications [16–18] and gives rise to some interesting electrochemical results when used as a layer on Pt surfaces. $PVF^+ClO_4^-$ electroactive film can act as a modified surface through which an electron transfer between a substrate and a reactant can take place. Studies related to the reduction and oxidation of some reactants through the polymer film-covered surface have been reported [19–21]. Also, It has been reported that $PVF^+ClO_4^-$ matrix is selective to the anions

* Corresponding author. Tel.: +90 332 2233877.
E-mail address: salihzekibas@gmail.com (S.Z. Baş).

1381-1177/$ – see front matter © 2011 Elsevier B.V. All rights reserved.
doi:10.1016/j.molcatb.2011.06.017

and some anions can be inserted into the polymer through an anion-exchange process [21]. The interaction between the negatively charged enzyme molecules and the polymer matrix, which ensures that the enzyme is homogeneously immobilized in the polymer matrix, is as follows:

$$PVF^+ClO_4^- + E^- \rightarrow PVF^+E^- + ClO_4^-$$

By using an anion-exchange process, a mild method developed binding of enzymes on $PVF^+ClO_4^-$ modified electrodes has been successfully applied to the design of the enzyme electrodes for glucose [22], sucrose [23], galactose [24], lactose [25], alcohol [26], choline [27] and acetyl choline [17]. In consideration of these electrodes prepared with different enzymes, the biocatalytical process for the oxidation of xanthine in the presence of XO can be summarized as following process:

The immobilized enzyme produces electroactive H_2O_2 as a result of following reaction with the substrate,

$$\text{xanthine} + O_2 + H_2O \xrightarrow{XO} \text{uric acid} + H_2O_2$$

H_2O_2 could be electrooxidized at the applied potential of +0.70 V versus SCE according to

$$H_2O_2 \rightarrow O_2 + 2H^+ + 2e^-$$

The oxidation of H_2O_2 could also occur chemically by the polyvinylferrocenium according to the following reaction.

$$H_2O_2 + 2PVF^+ \rightarrow O_2 + 2PVF + 2H^+$$

Amperometric response of the electrode was further enhanced as a result of the catalytic regeneration of PVF^+ sites at the same applied potential

$$PVF \rightarrow PVF^+ + e^-$$

H_2O_2 can be oxidized both electrochemically at the applied potential and chemically by the PVF^+ sites on the PVF^+ coated electrodes.

Metal particles used as electrode modified materials have attracted much attention in electrochemical applications, recently [28–30]. The previous studies indicated that platinum nanoparticles could increase the surface area and conducive to electron transfer with strong catalytic properties [31]. Nano-structured Pt modified electrodes have been frequently used to design amperometric biosensors based on the detection of hydrogen peroxide released during the oxidation of the substrate by an enzyme in the presence of oxygen. For example, Zou et al. [32] reported a novel glucose biosensor based on electrodeposition of platinum nanoparticles onto multi-walled carbon nanotube, and the prepared biosensor exhibited excellent electrocatalytic activity towards H_2O_2 electrooxidation and high stability. Chu et al. [33] developed a new amperometric biosensor based on adsorption of glucose oxidase at the gold and platinum nanoparticles modified carbon nanotube electrode, and the enzyme electrode exhibited good catalytic activity to the electrooxidation of H_2O_2.

In this study, we reported fabrication, characterization and analytical performance of xanthine biosensors prepared by immobilizing xanthine oxidase on $PVF^+ClO_4^-$ electrode and based on electrodeposition of Pt nanoparticles onto the surface of $PVF^+ClO_4^-$ electrode. The changes in the response of the enzyme electrode with various parameters such as substrate and enzyme concentrations, applied potential, polymeric film thickness, immobilization time of enzyme and temperature were established. The influence of electrodeposition potential, amount of electrodeposited Pt nanoparticles and H_2PtCl_6 concentration on the biosensor performance were also evaluated. The results showed that the biosensors exhibited high sensitivity, good reproducibility, extended linearity and freedom of interference from uric acid and ascorbic acid.

2. Experimental

2.1. Reagents

Xanthine oxidase (EC 1.17.3.2, Fluka-86106) and xanthine (Fluka-X0626) were purchased from Sigma (St. Louis, MO, USA). The enzyme solution was prepared by dissolving of XO in 0.01 M phosphate buffer solution (PBS) of pH 7.4, and stored at 4 °C. Xanthine solution was prepared in 0.1 M PBS of pH 7.4. PBS was prepared using NaH_2PO_4 (Merck, Darmstadt, Germany) and NaOH (Merck, Darmstadt, Germany), and adjusted with NaOH or H_3PO_4 (Merck, Darmstadt, Germany) to various pH values. PVF was prepared using a method of chemical polymerization [34] of vinylferrocene (Alfa Aesar, Ward Hill, MA, USA). Tetrabutylammonium perchlorate (TBAP) was prepared by the reaction of tetrabutylammonium hydroxide (Fluka, ~40% aqueous solution, St. Louis, MO, USA) with $HClO_4$ (Analar BDH, %70, Poole, UK), and crystallized from an ethanol–water mixture (9:1) several times and then, kept under nitrogen atmosphere after vacuum drying at 120 °C. H_2PtCl_6 solution was prepared by dissolving H_2PtCl_6 (Alfa Aesar, Ward Hill, MA, USA) in 0.5 M HCl solution. The purification of methylene chloride (Merck, Darmstadt, Germany) was accomplished according to the method proposed in literature [35]. All aqueous solutions were prepared in deionized water.

2.2. Measurements and apparatus

The response currents of xanthine electrodes were measured in a thermostated cell at the desired temperature, containing 0.1 M PBS, pH 7.4. The buffer solution in this cell was saturated with oxygen gas at a constant flow rate to obtain an oxygen saturated solution. In order to determine the steady-state background current of the enzyme electrode, a potential of +0.50 V versus SCE was applied to the enzyme electrode in 0.1 M PBS that did not contain xanthine. After the steady-state current value had been determined, known amounts of xanthine were added to the cell from a stock xanthine solution and the solution was stirred for 2–3 s. The xanthine response of the enzyme electrode was amperometically measured at a constant potential of +0.50 V versus SCE due to the electrooxidation of H_2O_2 produced enzymatically.

All electrochemical measurements were carried out in a conventional three-electrode system. The reference electrodes were non-aqueous Ag/AgCl in electroprecipitation, and SCE for xanthine analysis and Pt electrodeposition. Pt spiral electrode was used as the counter electrode. The working electrode was a platinum disc electrode (area: 0.0314 cm^2). Pt disc electrode was polished first with 0.3–0.05 μm alumina powder on a wet polishing pad. Then, Pt electrode was rinsed with deionized water and dried in air. The electrochemical studies were performed with an CHI-660C (Shanghai CH Instruments Co., China) electrochemical workstation. Scanning electron microscopy (SEM) images were obtained by using EVO-LS 10 (Carl Zeiss, Germany).

2.3. Preparation of PVF^+XO^- and PVF^+XO^-/Pt

$PVF^+ClO_4^-$ was electroprecipitated on a platinum electrode by electrooxidizing PVF at +0.7 V versus an Ag/AgCl electrode in methylene chloride solution containing 0.1 M TBAP. The electroprecipitation of $PVF^+ClO_4^-$ was carried out under nitrogen atmosphere. The thicknesses of polymer film were controlled by the electrical charge passed during the electroprecipitation of $PVF^+ClO_4^-$. The first biosensor developed in this study is based on immobilization of XO on $PVF^+ClO_4^-$ coated Pt electrode. The

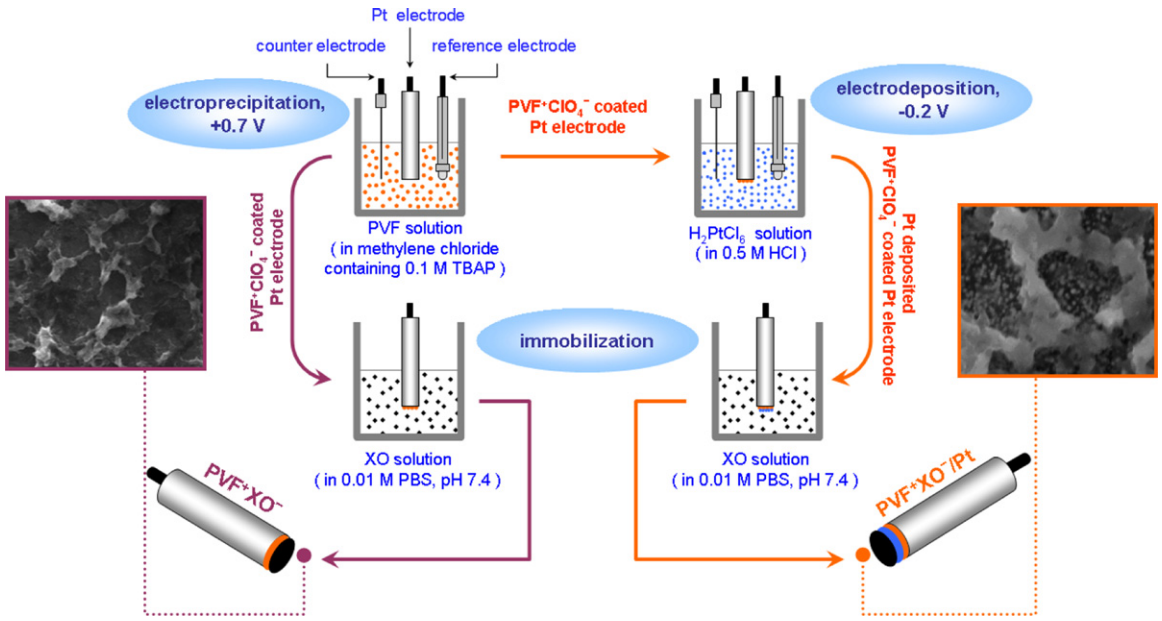

Fig. 1. A schematic showing the steps involved in the fabrication of PVF^+XO^- and PVF^+XO^-/Pt electrodes.

biosensor was prepared by immersing $PVF^+ClO_4^-$ coated Pt electrode in XO solution, and this biosensor was called as PVF^+XO^- electrode. The preparation of PVF^+XO^- electrode was schematically shown in Fig. 1. The polymer-coated electrode was kept in the enzyme solution for certain times without stirring (the optimized immobilization time: 20 min). The pH of the enzyme solution was kept above the isoelectric point (between pH 5.3 and 5.4) of XO. The enzyme molecule exists in the form of an anion (XO^-) under these conditions, facilitating its interaction with the oxidized polymer. The enzyme electrode was rinsed with 0.01 M PBS of pH 7.4 to remove the excess enzyme not held electrostatically, and then stored at 4 °C in 0.01 M PBS (pH 7.4) prior to use. The second biosensor is based on electrodeposition of Pt nanoparticles onto the surface of $PVF^+ClO_4^-$ coated Pt electrode and this biosensor was called as PVF^+XO^-/Pt electrode. The preparation procedure of PVF^+XO^-/Pt electrode was shown in Fig. 1. Electrodeposition of platinum on $PVF^+ClO_4^-$ coated Pt electrode was performed in an electroplating bath consisted of 2 mM H_2PtCl_6 and 0.5 M HCl. The $PVF^+ClO_4^-$ modified electrode was immersed in the plating bath and a constant potential of −0.20 V was applied for certain time. After the electrodeposition, the electrode was thoroughly rinsed with deionized water. The amount of loaded Pt nanoparticles on the modified electrode was evaluated from the electrical charge consumed during electrodeposition, assuming that Pt^{4+} to Pt^0 reduction is 100% efficient [32]. Then, the platinum electrodeposited $PVF^+ClO_4^-$ coated electrode was immersed in XO solution without stirring for 20 min for the immobilization of XO. The enzyme electrode were washed with 0.01 M PBS (pH 7.4) to remove the excess enzyme and stored at 4 °C in 0.01 M PBS.

3. Results and discussion

3.1. SEM images and cyclic voltammograms of PVF^+XO^- and PVF^+XO^-/Pt

Fig. 2 shows typical cyclic voltammograms of the enzyme electrodes in the absence and presence of xanthine. In the presence of xanthine, the cyclic voltammograms of both electrodes displayed an enhancement of the anodic peak current. It can be seen that the peak current value obtained from the PVF^+XO^-/Pt electrode is substantially higher than that of the PVF^+XO^- electrode. This observation demonstrated the electrocatalytic effect of Pt nanoparticles in the polymer matrix. Also, the effects of the scan rate on the peak current were studied to determine the type controlled process of the enzyme electrodes. Figs. S1A and S1B (Supporting information) show the plots of the anodic peak currents of the PVF^+XO^- and PVF^+XO^-/Pt electrodes vs. scan rate (10–1000 mV s^{-1}) with correlation coefficients of 0.9978 and 0.9983. The anodic peak currents of the electrodes are linearly proportional to the lower scan rates between 10 and 300 mV s^{-1}, indicating that the redox behaviors of the electrodes are surface controlled process as expected for immobilized systems. Figs. S1C and S1D (Supporting information) show the changes of the anodic peak currents of the enzyme electrodes with the square root of the scan rate (10–1000 mV s^{-1}) with correlation coefficients of 0.9980 and 0.9984. The plots of the anodic peak current against the square root of the higher scan rate ranging from 300 to 1000 mV s^{-1} demonstrate the strong linear relationships for PVF^+XO^- and PVF^+XO^-/Pt electrodes. These results indicate that the redox behaviors of the electrodes at the higher scan rate are diffusion controlled.

The morphologies of $PVF^+ClO_4^-$, PVF^+XO^- and PVF^+XO^-/Pt electrodes were also characterized by scanning electron microscopy (Fig. 3). As shown in Fig. 3A, the polymer film has suitable surface area which provides an ideal matrix for the electrodeposition of Pt and the immobilization of enzyme. After XO incorporated into $PVF^+ClO_4^-$ matrix via ion exchange process, the enzyme was observed at the vicinity of the surface of PVF^+ film (Fig. 3B). SEM image of PVF^+XO^-/Pt is shown in Fig. 3C. The platinum nanoparticles, with a diameter ranging from 40 nm to 70 nm, exhibit uniform size and semispherical shape, and appear regularly distributed over the polymer surface.

3.2. Response characteristics of PVF^+XO^- and PVF^+XO^-/Pt

Fig. 4A and B shows current–time plots for PVF^+XO^- and PVF^+XO^-/Pt electrodes under the optimal conditions with successive additions of 0.1 mM xanthine solutions to a stirred PBS (0.1 M, pH 7.4). As a result of the enzymatic reaction occurred between XO and xanthine, the response current of the enzyme electrodes increased gradually with stepped increasing of xanthine concentration in PBS. The current signal of PVF^+XO^-/Pt electrode is higher than that of PVF^+XO^- electrode due to the electrocatalytic effect of

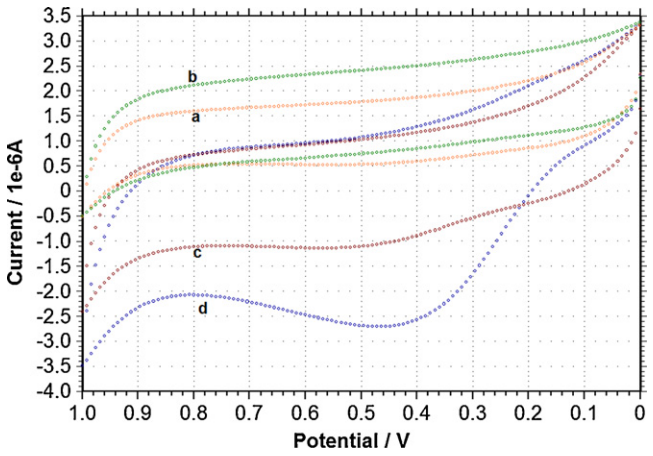

Fig. 2. Cyclic voltammograms of enzyme electrodes: (a) PVF^+XO^-, (b) PVF^+XO^-/Pt in absence of xanthine, (c) PVF^+XO^- in presence of 1.00 mM xanthine, and (d) PVF^+XO^-/Pt in presence of 1.00 mM xanthine in 0.1 M PBS (pH 7.4). Scan rate: 50 mV s^{-1}.

Pt nanoparticles. The response time of PVF^+XO^-/Pt electrode was determined as 15 s while the response time of PVF^+XO^- electrode is 10 s (reaching 90% of the maximum responses). It is possible that the electrodeposition of platinum at the electrode surface caused the limited diffusion rate of xanthine from bulk solution into the polymeric matrix.

3.3. Effect of applied potential

The effect of applied potential on the response currents of PVF^+XO^- electrode to xanthine was examined at different potentials between 0.2 and 0.8 V. With the increase of the applied potential from 0.2 V to 0.5 V, the response current increased regularly. When the applied potential was higher than 0.5 V, the response currents fell down. In the same way, the response currents of PVF^+XO^-/Pt electrode were studied at different potentials and a maximum response current was observed at 0.5 V as in PVF^+XO^- electrode. This means that the response currents of the biosensors are resulted from the electrochemical oxidation of hydrogen peroxide. Thus, a potential of 0.5 V was preferred for xanthine detection in the following experiments.

3.4. Effect of polymeric film thickness

The effect of the polymeric film thickness on the response current was examined using $PVF^+ClO_4^-$ films with various thicknesses. When the enzyme concentration was kept constant (1.0 mg mL^{-1} for XO), the charge that passed in the preparation of the polymer coated electrodes varied between 0.5 and 4.5 mC corresponding to 1.650×10^{-7} mol cm^{-2} of PVF^+ and 1.485×10^{-6} mol cm^{-2} of PVF^+. The enzyme electrode response increased with the polymer thickness up to a value 2.5 mC corresponding to 4.950×10^{-7} mol cm^{-2} of PVF^+ and then, decreased slowly. This behavior could be explained by the limited diffusion rate of xanthine from the bulk solution into the inner regions of the polymer in thick film [21]. The thickness of the $PVF^+ClO_4^-$ film was kept constant at this value for all measurements.

3.5. Effects of XO concentration and immobilization time

The amount of the enzyme in polymer matrix depends on the immobilization time of enzyme and the concentration of the enzyme solution used during immobilization process. To investigate the effect of the enzyme concentration on the response

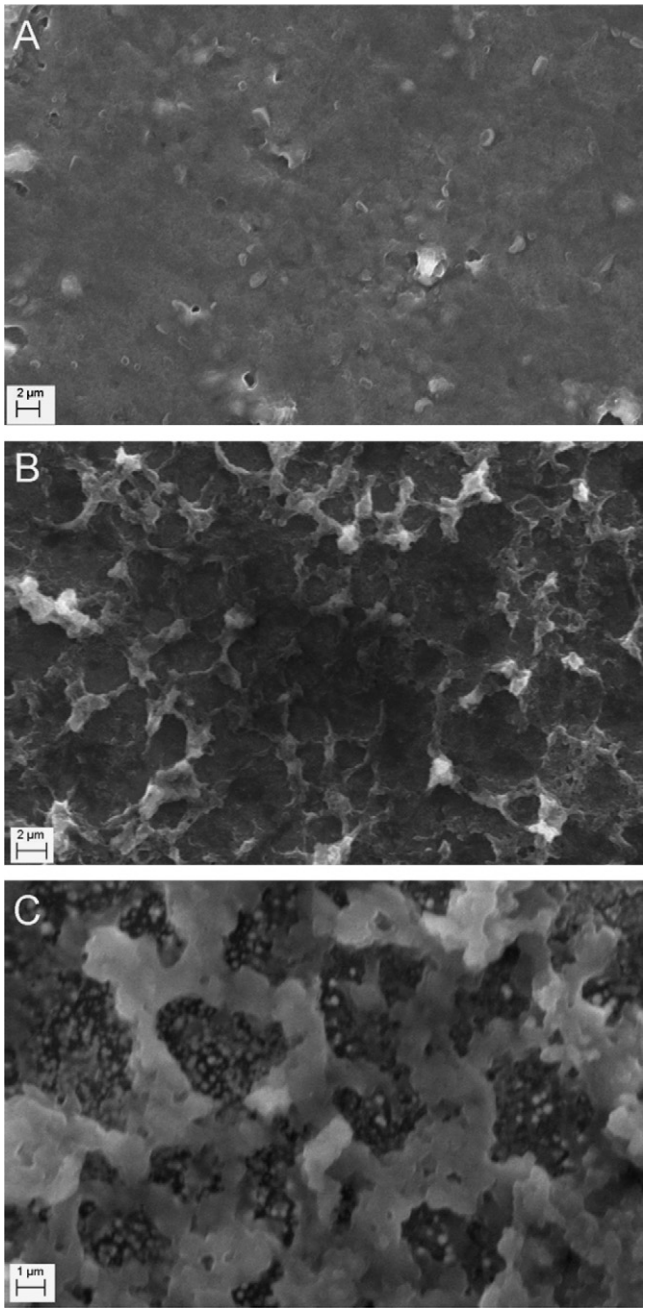

Fig. 3. SEM images of modified electrodes: (A) $PVF^+ClO_4^-$, (B) PVF^+XO^-, and (C) PVF^+XO^-/Pt.

current, the enzyme electrodes were prepared with the XO concentrations varying between 0.5 and 8.0 mg mL^{-1}. With the increase of the XO concentration from 0.5 mg mL^{-1} to 1.5 mg mL^{-1}, the response current of PVF^+XO^- electrode increased accordingly, which implies that higher XO concentration resulted in higher sensitivity. When the concentration of XO was higher than 1.5 mg mL^{-1}, the response current did not change appreciably (Fig. S2A (Supporting information)). This result is consistent with the previous studies [26,27,36]. The optimum bulk enzyme concentration for the enzyme immobilization was determined as 1.5 mg mL^{-1}. In addition to the optimization of XO concentration, the effect of the different immobilization time of XO on the current response was investigated. The maximum current value was obtained at the immobilization time of 20 min and then, the current value reached a plateau (Fig. S2B (Supporting information)).

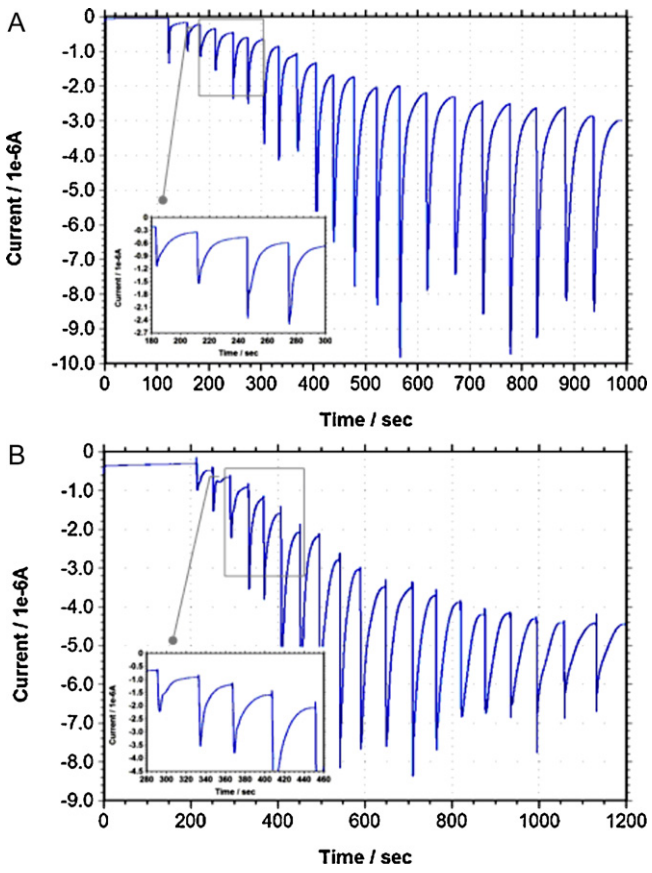

Fig. 4. Amperometric responses of enzyme electrodes with successive addition of 0.1 M xanthine in 0.1 M PBS (pH 7.4) at the applied potential of 0.5 V: (A) PVF^+XO^- and (B) PVF^+XO^-/Pt.

Therefore, the immobilization time of 20 min was selected in all of measurements.

3.6. Effect of Pt electrodeposition potential

The effect of the electrodeposition potential of Pt nanoparticles on the current response of PVF^+XO^-/Pt was tested with the biosensors prepared at the potentials between −0.1 V and −0.6 V vs. Ag/AgCl. As illustrated in Fig. 5A, the current response gradually increased as the electrodeposition potential became more negative up to −0.2 V, reached a maximum at this potential and then, decreased for more negative potential values than −0.2 V. This result is similar to that reported for the electrodeposition potential of Pt by several researchers [37,38]. The deposition potential of −0.2 V was selected for Pt electrodeposition in the following experiments.

3.7. Effect of amount of electrodeposited Pt nanoparticles

The effect of the amount of electrodeposited Pt nanoparticles was studied by controlling the electrical charge consumed during the electrodeposition at −0.2 V. To compare the catalytic activities, PVF^+XO^-/Pt electrodes were prepared at the electrical charges varying between 0.5×10^{-2} C and 8.0×10^{-2} C during Pt electrodeposition on $PVF^+ClO_4^-$ film. The maximum response currents measured at 0.5 V in 0.1 M PBS (pH 7.4) were plotted versus charges for Pt electrodeposition as shown in Fig. 5B. The response current of PVF^+XO^-/Pt electrode increased with the increase of the charge from 0.5×10^{-2} C to 4.0×10^{-2} C and then, started to decrease with a charge of more than 4.0×10^{-2} C. This result may be attributed to the decrease of the electrochemical active surface area of the electrode because of large-sized Pt nanoparticles deposited on the electrode surface with a high charge [32,39,40]. Therefore, the charge of 4.0×10^{-2} C for Pt electrodeposition was used in all of measurements.

3.8. Effect of H_2PtCl_6 concentration

The effect of H_2PtCl_6 concentration for Pt electrodeposition was investigated using H_2PtCl_6 solution varying between 0.5 mM and 4.0 mM (Fig. 5C). It was observed that the response current of PVF^+XO^-/Pt electrode increased evidently with the increase of H_2PtCl_6 concentration from 0.5 mM to 2.0 mM. When the concentration of H_2PtCl_6 was higher than 2.0 mM, the response was decreased. It is clear that the increasing of H_2PtCl_6 concentration leads to a change of the platinum nanoparticle size and affect negatively to electrocatalytic activity [41]. Hence, the H_2PtCl_6 concentration was chosen as 2.0 mM and the Pt nanoparticle-based enzyme electrode were prepared on these conditions.

3.9. Effect of temperature

The effect of temperature on the response currents of the enzyme electrodes was determined at different temperatures varying from 20 to 60 °C. The response current of the PVF^+XO^- electrode increased with the increasing temperature from 20 to 40 °C and decreased at higher temperature. The activation energy for the PVF^+XO^- electrode was calculated to be 23.64 kJ mol^{-1} for the oxidation of xanthine. The activity of the PVF^+XO^-/Pt electrode reached a maximum value at about 45 °C and decreased after this temperature. The activation energy for the oxidation of xanthine on the PVF^+XO^-/Pt electrode was found to be 29.11 kJ mol^{-1} from Arrhenius plot. The decrease in the response currents of the enzyme electrodes at a higher temperature may have two reasons: one is the decreasing concentration of molecular oxygen in the solution, another is the thermal deactivation of the enzyme at higher temperatures [42]. In addition, it can be observed that heat resistance of the immobilized enzyme was increased slightly by the electrodeposition of Pt.

3.10. Reproducibility and stability

The reproducibility of both enzyme electrodes, PVF^+XO^- and PVF^+XO^-/Pt, was estimated from the response to 1.0 mM xanthine for five enzyme electrodes prepared under the optimum working conditions and the relative standard deviation (R.S.D.) is 3.30% for PVF^+XO^- and 5.76% for PVF^+XO^-/Pt. The storage stability of PVF^+XO^- and PVF^+XO^-/Pt electrodes was also studied. The storage stability of the enzyme electrodes was determined by measuring steady-state response current of 1.0 mM xanthine during 40 days. The PVF^+XO^- electrode exhibited good stability during 10 days and then an activity loss of 40% was observed on the 21st day. The lifetime of PVF^+XO^-/Pt electrode is slightly longer than the PVF^+XO^- electrode and the current response of PVF^+XO^-/Pt on the 25th days was 42% of the initial value. Such good stability of PVF^+XO^-/Pt may be attributed to the aspect that Pt nanoparticles–polymer matrix was stable.

3.11. Effect of substrate concentration

Fig. 6A and B shows the calibration curves of both electrodes. The response current of PVF^+XO^- electrode is linear in the range from 1.73×10^{-3} to 1.74 mM with a correlation coefficient of 0.9996 (Fig. 6A). The sensitivity is 56.22 μA mM^{-1} cm^{-2} for xanthine. Compared with $PVF+XO^-$ electrode, PVF^+XO^-/Pt electrode exhibits wide linear range from 0.43×10^{-3} to 2.84 mM with a correlation

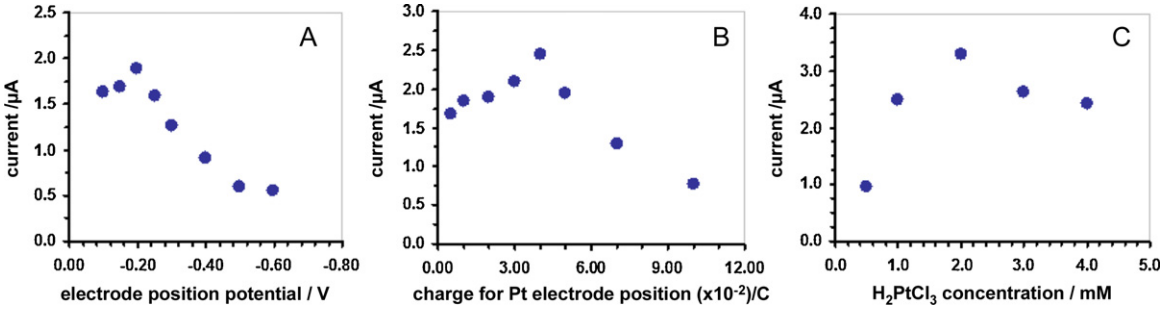

Fig. 5. The effects of electrodeposition potential (A), passing charge during Pt electrodeposition (B), H_2PtCl_6 concentration (C) on the amperometric response of PVF^+XO^-/Pt electrode.

coefficient of 0.9989 (Fig. 6B). The linear ranges of PVF + XO^- and PVF^+XO^-/Pt electrodes are wider than many of those reported in literature [10,13,43,44]. The PVF^+XO^-/Pt electrode has a sensitivity of 68.75 µA mM^{-1} cm^{-2}. For both enzyme electrodes, PVF^+XO^- and PVF + XO^-/Pt, the detection limits were found to be 5.20×10^{-4} mM and 1.30×10^{-4} mM at the signal-to-noise ratio of 3 (S/N = 3), respectively. The detection limits of PVF^+XO^- and PVF + XO^-/Pt are lower than that of polypyrrole modified film (1.0×10^{-3} mM) [45], ZnO–NPs–polypyrrole composite film (8.0×10^{-4} mM) [46] but higher than that of laponite thin film (1.0×10^{-5} mM) [11], multi-wall carbon nanotubes (1.0×10^{-4} mM) [13].

The apparent Michaelis–Menten constant (K_{mapp}) can be calculated from the electrochemical version of the Linweaver–Burk equation as suggested by Shu and Wilson [47]:

$$\frac{1}{i_s} = \frac{1}{i_{max}} + \frac{K_{mapp}}{i_{max}} \frac{1}{C}$$

where i_s is the steady-state current, i_{max} is the maximum current, K_{mapp} the apparent Michaelis–Menten constant, C is the concentration of xanthine. According to the Lineweaver–Burk equation, K_{mapp} values of the enzyme electrodes can be obtained from the analysis of the slope and the intercept of the plot of the reciprocals of the steady-state current versus xanthine concentration. K_{mapp} values were found to be 6.065 mM and 3.454 mM xanthine for PVF^+XO^- and PVF^+XO^-/Pt electrodes, respectively.

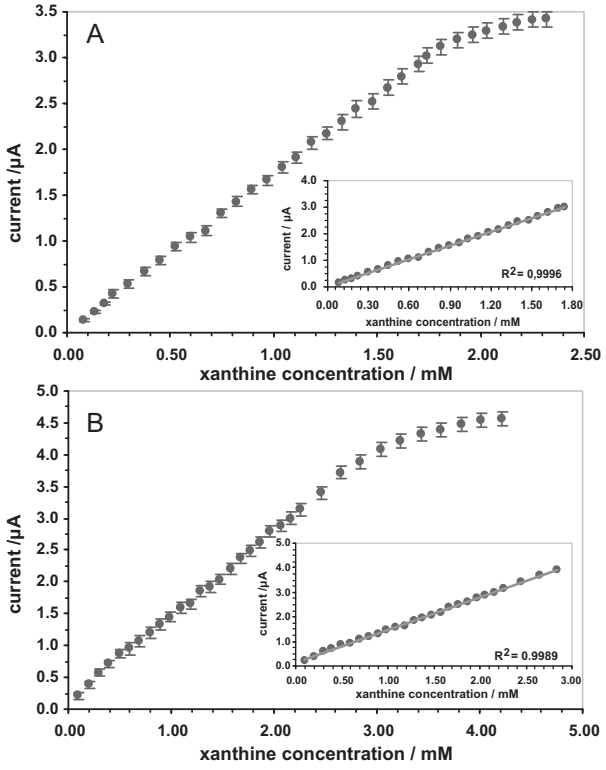

Fig. 6. Calibration curves of enzyme electrodes for xanthine determination: (A) PVF^+XO^- and (B) PVF^+XO^-/Pt.

3.12. Interference study

The effect of possible interfering substances on PVF^+XO^- and PVF^+XO^-/Pt electrodes was investigated by using ascorbic acid and uric acid at 0.50 V (versus SCE) in 0.10 M PBS (pH 7.4). The current responses obtained in the presence of interfering species at their physiological normal level (0.1 mM ascorbic acid, 0.5 mM uric acid) [48] were compared with those obtained in 0.5 mM xanthine solution. No noticeable changes in the current responses were detected in the ascorbic acid solution. A similar situation was observed for 0.5 mM uric acid solution. These results indicated that both biosensors have acceptable anti-interferent ability.

3.13. Real sample analysis

The antiasthmatic drugs containing xanthine derivatives such as teophylline and aminophylline are used in the treatment of patients with respiratory distress syndrome. In the analysis of real samples, the two different drugs were assayed to demonstrate the practical use of PVF^+XO^- and PVF^+XO^-/Pt electrodes. The results of the xanthine determination and the recovery of the drug samples using both electrodes were summarized in Table S1 (Supporting information). The results obtained are satisfactory and agree closely with those given by the prospectuses of the drugs.

4. Conclusion

In this paper, two novel amperometric biosensors for monitoring xanthine were described and characterized. The former was prepared by immobilization of XO on $PVF^+ClO_4^-$ matrix. The other constructed by electrodeposition of Pt nanoparticles on the $PVF^+ClO_4^-$ matrix, and then the enzyme was immobilized onto $PVF^+ClO_4^-$/Pt electrode surfaces. In our amperometric measurements, we observed that deposited Pt nanoparticles on $PVF^+ClO_4^-$ matrix provide significant electrocatalytic activity towards hydrogen peroxide oxidation. Compared with the PVF^+XO^- electrode, the PVF^+XO^-/Pt electrode has larger maximum current density, higher sensitivity and a wider linear response range. Both enzyme electrodes also demonstrated good stability and non-interferences. The results obtained may be attributed to the catalytic effect of Pt nanoparticles and the good biocompatibility of $PVF^+ClO_4^-$ matrix. As a conclusion, the enzyme electrodes fabricated in this study can be a good example for designing a variety of bioelectrochemical devices with a wide linear range and high sensitivity.

Acknowledgements

The authors are grateful for the financial support provided by the Selçuk University Research Foundation (BAP) under Project 08101018.

Appendix A. Supplementary data

Supplementary data associated with this article can be found, in the online version, at doi:10.1016/j.molcatb.2011.06.017.

References

[1] R. Hille, Arch. Biochem. Biophys. 433 (2005) 107–116.
[2] X. Liu, W.M. Lin, X.H. Yan, X.H. Chen, J.R. Hoidal, P. Xu, J. Chromatogr. B 785 (1998) 101–114.
[3] R. Harrison, Free Radic. Biol. Med. 33 (2002) 774–797.
[4] D. Shan, Y. Wang, M. Zhu, H. Xue, S. Cosnier, C. Wang, Biosens. Bioelectron. 24 (2009) 1171–1176.
[5] D. Shan, Y. Wang, H. Xue, S. Cosnier, Sens. Actuators B 136 (2009) 510–515.
[6] T. Richter, L.L. Shultz-Lockyear, R.D. Oleschuk, U. Bilitewski, D.J. Harrison, Sens. Actuators B 81 (2002) 369–376.
[7] E. Causse, A. Pradelles, B. Dirat, A. Negre-Salvayre, R. Salvayre, F. Couderc, Electrophoresis 28 (2007) 381–387.
[8] M. Czauderna, J. Kowalczyk, J. Chromatogr. B 744 (2000) 129–138.
[9] N. Cooper, R. Khosravan, C. Erdmann, J. Fiene, J.W. Lee, J. Chromatogr. B 837 (2006) 1–10.
[10] Ü.A. Kirgöz, S. Timur, J. Wang, A. Telefoncu, Electrochem. Commun. 6 (2004) 913–916.
[11] D. Shan, Y.N. Wang, H.G. Xue, S. Cosnier, S.N. Ding, Biosens. Bioelectron. 24 (2009) 3556–3561.
[12] R. Villalonga, M. Matos, R. Cao, Electrochem. Commun. 9 (2007) 454–458.
[13] Y. Gao, C. Shen, J. Di, Y. Tu, Mater. Sci. Eng. C 29 (2009) 2213–2216.
[14] A.T. Lawal, S.B. Adeloju, J. Mol. Catal. B 66 (2010) 270–275.
[15] M. Şenel, E. Çevik, M.F. Abasıyanık, Sens. Actuators B 145 (2010) 444–450.
[16] H. Patel, X. Li, H.I. Karan, Biosens. Bioelectron. 18 (2003) 1073–1076.
[17] S. Şen, A. Gülce, H. Gülce, Biosens. Bioelectron. 19 (2004) 1261–1268.
[18] F. Kuralay, H. Özyörük, A. Yıldız, Sens. Actuators B 114 (2006) 500–506.
[19] H. Gülce, H. Özyörük, A. Yıldız, Ber. Bunsenges. Phys. Chem. 98 (1994) 228–233.
[20] H. Gülce, H. Özyörük, A. Yıldız, Ber. Bunsenges. Phys. Chem. 98 (1994) 828–832.
[21] H. Gülce, H. Özyörük, A. Yıldız, Electroanalysis 7 (1995) 178–183.
[22] H. Gülce, H. Özyörük, S.S. Çelebi, A. Yıldız, J. Electroanal. Chem. 394 (1995) 63–70.
[23] H. Gülce, H. Özyörük, S.S. Çelebi, A. Yıldız, J. Electroanal. Chem. 397 (1995) 217–223.
[24] H. Gülce, İ. Ataman, A. Gülce, A. Yıldız, Enzyme Microb. Technol. 30 (2002) 41–44.
[25] H. Gülce, A. Gülce, A. Yıldız, Anal. Sci. 18 (2002) 1–3.
[26] H. Gülce, A. Gülce, M. Kavanoz, H. Coşkun, A. Yıldız, Biosens. Bioelectron. 17 (2002) 517–521.
[27] H. Gülce, Y.S. Aktaş, A. Gülce, A. Yıldız, Enzyme Microb. Technol. 32 (2003) 895–899.
[28] C.H. Lee, S.C. Wang, C.J. Yuan, K.C. Chang, Biosens. Bioelectron. 22 (2007) 877–884.
[29] Y. Velichkova, Y. Ivanov, I. Marinov, R. Ramesh, N.R. Kamini, N. Dimcheva, E. Horozova, T. Godjevargova, J. Mol. Catal. B 69 (2010) 168–175.
[30] J. Li, R. Yuan, Y. Chai, X. Che, J. Mol. Catal. B 66 (2010) 8–14.
[31] Z. Wang, F.A. Xu, Q. Yang, J.H. Yu, W. Huang, Y. Zhao, Colloid Surf. B 76 (2010) 370–374.
[32] Y. Zou, C. Xiang, L. Sun, F. Xu, Biosens. Bioelectron. 23 (2008) 1010–1016.
[33] X. Chu, D. Duan, G. Shen, R. Yu, Talanta 71 (2007) 2040–2047.
[34] T.W. Smith, J.E. Kuder, D. Wychick, J. Polym. Sci. 14 (1976) 2433–2448.
[35] D.D. Perrin, W.L.F. Armorego, Purification of Laboratory Chemicals, Pergamon Press, Oxford, 1980.
[36] B.C. Özer, H. Özyörük, S.S. Çelebi, A. Yıldız, Enzyme Microb. Technol. 40 (2007) 262–265.
[37] C.S. Kim, S.M. Oh, Electrochim. Acta 41 (1996) 2433–2439.
[38] Z. Lin, L. Ji, X. Zhang, Mater. Lett. 63 (2009) 2115–2118.
[39] H. Wu, J. Wang, X. Kang, C. Wang, D. Wang, J. Liu, I.A. Aksay, Y. Lin, Talanta 80 (2009) 403–406.
[40] G. Lu, G. Zangari, Electrochim. Acta 51 (2006) 2531–2538.
[41] Y. Huang, Q. Wen, J.H. Jiang, G.L. Shen, R.Q. Yu, Biosens. Bioelectron. 24 (2008) 600–605.
[42] J. Pei, X.Y. Li, Anal. Chim. Acta 414 (2000) 205–213.
[43] Y. Liu, L. Nie, W. Tao, S. Yao, Electroanalysis 16 (2004) 1271–1278.
[44] M. Çubukçu, S. Timur, Ü. Anik, Talanta 74 (2007) 434–439.
[45] F. Arslan, A. Yasar, F. Kılıç, Artif. Cell Blood Sub. 34 (2006) 113–128.
[46] R. Devi, M. Thakur, C.S. Pundir, Biosens. Bioelectron. 26 (2011) 3420–3426.
[47] F.R. Shu, G.S. Wilson, Anal. Chem. 48 (1976) 1679–1686.
[48] A.E.G. Cass, G. Davis, D.G. Francis, H.A.O. Hill, W.J. Aston, L.J. Higgins, E.V. Plotkin, L.D.L. Scott, A.P.F. Turner, Anal. Chem. 56 (1984) 667–671.